Influence of Electrochemical Discharge Machining Parameters on Machining Quality of Microstructure

Douyan Zhao
Laser Technology Institute, School of Mechanical Engineering, Jiangsu University
Hao Zhu
Laser Technology Institute, School of Mechanical Engineering, Jiangsu University
zhaoyang zhang (610591875@qq.com)
Laser Technology Institute, School of Mechanical Engineering, Jiangsu University
Kun Xu
Laser Technology Institute, School of Mechanical Engineering, Jiangsu University
Jian Gao
Laser Technology Institute, School of Mechanical Engineering, Jiangsu University
Xueren Dai
Laser Technology Institute, School of Mechanical Engineering, Jiangsu University
Lei Huang
Huibang Automation System Co., Ltd, Suzhou

Research Article

Keywords: Electrochemical discharge machining, Glass, Micro-hole, Microgroove, 3D microstructure

Posted Date: July 8th, 2021

DOI: https://doi.org/10.21203/rs.3.rs-670539/v1

Version of Record: A version of this preprint was published at The International Journal of Advanced Manufacturing Technology on November 9th, 2021. See the published version at https://doi.org/10.1007/s00170-021-08316-4.

Influence of electrochemical discharge machining parameters on machining quality of microstructure

Douyan Zhao[1], Hao Zhu[1], Zhaoyang Zhang[1*], Kun Xu[1], Jian Gao[1], Xueren Dai[1] and Lei Huang[2]

[1] Laser Technology Institute, School of Mechanical Engineering, Jiangsu University, Zhenjiang 212013, China
[2] Huibang Automation System Co., Ltd, Suzhou 215002, China

E-mail: zzhaoyang@126.com (Z. Zhang)

Abstract

As a nontraditional processing technology, Electrochemical discharge machining (ECDM) can precisely process glass and engineering ceramics. This technology has proven to be a potential process for glass 3D microstructure. However, the key to expanding the application of ECDM is how to improve machining accuracy. This research conducted micro-hole and microgroove machining. The influence of power voltage and frequency on hole processing efficiency, hole entrance diameter and hole limit depth explored. We considered four factors affecting ECDM--the voltage and frequency of the pulse power supply, the tool electrode feed rate, and the rotation speed. We studied their influence on the roughness of the microgrooves. The results show that machining efficiency, entrance diameter and limit depth of micro-holes increased with the increase in voltage, but decreased with the increase in power frequency. The results show that the roughness of microgrooves has an obvious positive correlation with the power voltage, while it had an obvious negative correlation with the power frequency and the electrode speed. The bottom surface roughness of microgrooves can be as small as 0.605μm. Various complex 3D microstructures on the glass surface by layer-by-layer method, which proved the great potential of ECDM.

Keywords: Electrochemical discharge machining, Glass, Micro-hole, Microgroove, 3D microstructure

Declarations

Funding: This work was supported by National Natural Science Foundation of China, grant number 52075227, 51905226; China Postdoctoral Science Foundation 2018M640461, 2019T120392; Natural Science Foundation of Jiangsu Province, grant number BK20180873, BK20180875; Postgraduate Research & Practice Innovation Program of Jiangsu Province 5561110037.
Conflicts of interest/Competing interests: The authors have no relevant financial or non-financial interests to disclose.
Availability of data and material: Not applicable
Code availability: Not applicable
Authors' contributions: Zhao Douyan: Conceptualization, Methodology, Writing-Original draft preparation.
Zhu Hao: Data curation.
Zhang Zhaoyang: Writing-Reviewing and Editing.
Xu Kun: Visualization.
Gao Jian: Supervision.
Dai Xueren: Validation
Huang Lei: Investigation

1. Introduction

Insulating and hard-brittle materials such as glass is widely used in Micro-Electro-Mechanical System (MEMS) because of their excellent chemical and physical properties. However, the hardness and brittleness of glass dampens its micro-fabrication. To achieve better processing quality and efficiency, scholars from various countries have developed many processing methods in recent years, including laser processing [1-3], chemical etching [4], ultrasonic processing [5] and so on. Laser processing can micro-process hard and brittle materials with high efficiency. However, the equipment is expensive and the high-energy density easily forms micro-cracks on the workpiece surface. Chemical etching techniques (such as HF etching) can provide excellent processing accuracy and fine clarity. However, complex processing, low etching rate and high environmental requirements limit its popularity. Ultrasonic processing is also suitable for processing hard and brittle materials, with a high material removal rate (MRR) and good surface integrity. However, due to the high frequency action of mechanical force, it is easy to cause micro-cracks and the processing tools wear quickly. Compared with the above nontraditional processes, ECDM needs simpler equipment and lower costs, and the machining process is more flexible [6-9]. These advantages make ECDM have great potential in processing nonconductive and hard-brittle materials.

ECDM has been studied for decades[10-15]. In ECDM, a tool electrode and an auxiliary electrode both immersed in the electrolyte, and the surface of the auxiliary electrode is much larger than that of the tool electrode. Connect the power source between tool electrode (cathode) and auxiliary electrode (anode), and bubbles will produce on the surface of tool electrode. As the reaction continues, the density of the bubbles increases and coalesces into a gas film that separates the electrode from the electrolyte. When the gas film electric field is high enough, it occurs electrical breakdown and produces much energy. The energy produces high temperature and high-pressure, which melts and throws out the material [16-18]. At the same time, the heat also promotes the chemical corrosion of the alkaline solution on the glass workpiece, and the two works together to achieve the material removal [19-20].

Kurafuji and Suda first proposed ECDM and used it to drill holes in glass [11], and scholars have gradually begun to study the machining of microgrooves. Later researchers applied ECDM in other materials and micro-manufacturing. Lijo Paul et al. [21] proved the material removal model and temperature model of ECDM. They found that the MRR and temperature range of pulse direct current (DC) power supply are better than DC power supply. Sumit et al. [22]studied the effect of tool electrode rotation, and found that proper rotation speed significantly improved the roundness of holes, but has no significant effect on the critical voltage and critical current. At the same time, the influence of NaOH concentration on the diameter of entrance and exit of holes explored, and found that both are proportional to the concentration. Jana et al. [23] studied the influence of electrolyte concentration, tool-surface gaps and power supply voltage on the surface texture of microgrooves, and obtained different surface textures of microgrooves by controlling the above parameters.

However, with the development of modern technology, it is necessary to process two-dimensional or even complex 3D structures on glass to meet application needs, which has high requirements for processing accuracy and surface roughness. For example, micro fluidic systems and micro reactors made of glass. However, not many studies on selecting proper parameters to machine complex 3D microstructures by exploring the effects of different experimental parameters of ECDM on the processing effects of micro-holes and microgrooves. Compared with the existing research, this article took into account the changes of the gas film in different processing processes, and used different processing methods in order to explore different focuses. When processing micro-holes, using gravity feed processing, the gas film is restricted by the hole wall, and the side of the gas film is subjected to the pressure of the hole wall. The MRR and limit depth are studied, and the influence of the overcut at the entrance is also explored. Uniform feed is used when machining microgrooves, because the side cutting is used, the force of the gas film is different from that of hole machining. At this time, the side of the gas film is mainly subjected to the pressure in the forward direction, and the bottom of the gas film receives the pressure from the bottom of the microgroove. The bottom surface roughness of the microgrooves was studied. Layer-by-layer processing is used when processing three-dimensional structures. When performing three-dimensional machining, at the first entry point of each layer, the force of the air film is the same as that of the hole, and the force of the subsequent air film is the same as that of the groove. Finally, combining the test results of micro-holes and microgrooves, selecting appropriate processing parameters to conduct a 3D processing experiment, and obtaining high-speed and high-quality processing results.

Compared with the existing research[24-25], this article has better economic benefits for effective processing at a lower voltage (17-25V). In this paper, the tool electrode used the electrode with thread on the surface, which is more conducive to the electrolyte circulation in the processing area.

2. Experimental design

2.1 Experimental setup

We designed and made an ECDM experiment device, as shown in Figure 1. The experiment equipment mainly included (a) the electrochemical discharge system, (b) the

detection system, and (c) the electrode movement system. The electrochemical discharge system mainly included a pulse DC power supply (GKPT series, Shenzhen Shicheng Electronic Technology Co., Ltd.), an auxiliary electrode (made of graphite block, size 80×20×15 mm^3), a tool electrode (made of tungsten carbide, R=0.1 mm) and a solution tank (made of acrylic plate, size 160×120×80 mm^3). The detection system mainly included an oscilloscope (1GHz bandwidth, 5GS/s sampling rate) and a current probe (CP8030B, Shenzhen Zhiyong Electronics Co., Ltd.). The current probe collected the current signal in the circuit, and displayed and recorded the waveform of the current signal on the oscilloscope. The electrode movement system mainly included an X-Y-Z three-axis motion processing platform, a rotating spindle, a computer and a motion controller. The processing platform realized X-Y-Z three-axis movement and rotation through a computer-controlled motion controller. The motion platform driver used 128 subdivisions. The step angle of the stepping motor was 1.8° and the lead of the X-Y-Z three-axis ball screw was 5 mm. So, the motion resolution of the three-axis CNC platform was 0.195 μm. That is, under a single pulse, the distance moved by any axis is only 0.195 μm, which can fully meet the needs of low-speed feed in the experiment.

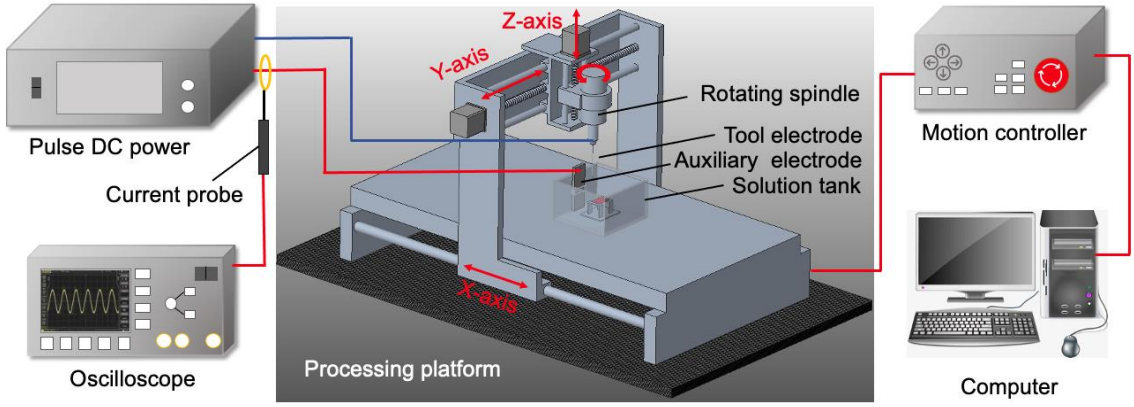

Figure 1. Schematic diagram of the experimental apparatus.

Table 1. The machining parameters of ECDM.

Parameters	Values
Solution	20 wt.% NaOH
Workpiece	Soda lime glass (size 30×30×2mm^3)
Tool electrode	Tungsten carbide (WC, R=0.1 mm)
Auxiliary electrode	Graphite block (size 80×20×15 mm^3)
Pulse duty cycle	50%
Tool immersion	2 mm

The solution tank fixed on the processing platform, and the workpiece was a square piece of soda lime glass with a size of 30×30×2mm^3, which fixed at the bottom of the solution tank by a bracket. The processing parameters are shown in Table 1.

2.2 Machining procedures

In this study, we systematically carried out experiments on machining micro-holes, microgrooves and 3D microstructures.

In the micro-hole experiment, we used a workpiece gravity feed system (Figure 2) for processing micro-holes, which composed of a digital dial indicator (Ace Instrument Co., Ltd.) and a pulley slider. The digital dial indicator was for detection of the processing depth of micro-holes during the experiment. The workpiece was clamped on the slide carriage, and the balancing weight pulled the slide carriage to move upward along the sliding rail. So, the workpiece and the tool electrode always keep contact. The balancing weight adjusted to keep a contact force of about 10 grams between the tool electrode and the workpiece. The head of the digital display dial indicator kept in contact with the balancing weight. During the micro-hole machining, the height of the balancing weight drops (that is, the machining depth of the workpiece) can display by the digital display dial indicator. Record the processing depth every 10 seconds (S) during the processing, and set the total processing time to 60 S. The difference of the processing depth recorded in two adjacent times divided by the time

period (10 seconds) is the MRR of this period of time. The tool electrode rotation speed was 1000 rpm.

During the electrochemical discharge micro-hole machining process, the average power consumed by the machining area P_0 is [26]:

$$P_0 = (U - U_d)\bar{I} - R\bar{I}^2 \quad (1)$$

In the formula, U is the output voltage of the power supply, U_d is the electrolyte decomposition voltage, $\bar{I}$ is the average current, and R equal the resistance between the two electrodes in the electrolyte.

Spark discharge occurred both the bottom of the electrode and the sidewall of the electrode. But only the spark discharge produced at the bottom of the electrode increase the depth of the micro-hole, while the spark discharge produced on the sidewall does not help the depth of the micro-hole. It increased the diameter of the micro-hole. During the processing, the power acting on the bottom of the micro-hole is:

$$P_b = \frac{\varepsilon - f t_1}{f}[(U - U_d)\bar{I} - R\bar{I}^2]\frac{A_b}{A_s} \quad (2)$$

where ε is the duty cycle of the output power supply, f is the power output frequency, t_1 is the formation time of the gas layer, A_b is the area of the bottom of the electrode, and A_s is the total area of the electrode immersed in the solution.

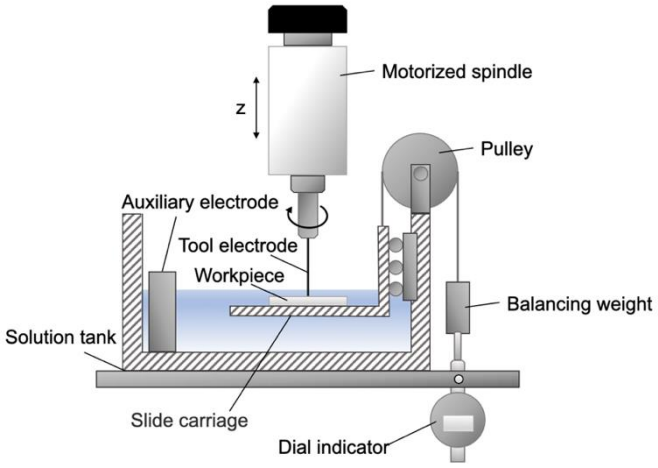

Figure 2. Schematic diagram of gravity feed system of ECDM micro-hole drilling.

It can conclude from Equation 2 that when the power frequency f is lower or the pulse voltage U is higher, the processing power at the bottom of the electrode will become larger, and the heat released each unit time will be more, so the processing speed and processing depth will increase.

When the depth of the processed micro-hole is small, the electrochemical discharge micro-hole processing speed is [27]:

$$v_k = \frac{2a}{b\sqrt{\pi}}\frac{1 - e^{-1/\bar{t_0}(k)}}{\sqrt{\bar{t_0}(k)}} \quad (3)$$

where $\bar{t_0} = t_0/\tau$, $\tau = b^2/4a$ is the thermal conductivity of the workpiece material, b is the radius of the heat source, t_0 is the initial temperature at the beginning of processing, k is the ratio between the heat source power P_0 and the minimum power required to remove material P_{min}.

Therefore, in the electrochemical discharge micro-hole machining process, the processing depth is:

$$z_k = \int_{t_1}^{t_2} \frac{2a}{b\sqrt{\pi}}\frac{1 - e^{-1/\bar{t_0}(k)}}{\sqrt{\bar{t_0}(k)}} \quad (4)$$

The above processing speed v_k and processing depth z_k are only applicable when the hole processing depth is shallow.

As micro-holes become deeper, circulating electrolyte in the hole becomes difficult [28-30]. Also, the bubbles produced by the electrolysis reaction will accumulate at the hole entrance, further hindering circulating electrolyte in the hole. It is difficult to form an effective spark discharge at the bottom of the electrode, resulting in a gradual decrease in MRR. Finally, when the electrolyte at the bottom of the hole consumed, the processing cannot continue and the depth of the micro-hole reaches a limit value. At the same time, the large store of bubbles at the entrance also makes the spark discharge in this area more intensive, which increase the diameter of the entrance and produce cracks on the surface.

According to the formula, voltage and frequency are the main influencing factors. So, we experimented with these parameters. Table 2 shows the variation of processing parameters in micro-hole experiment.

Table 2. The machining parameters used in the machining micro-hole experiment.

Group	Voltage(V)	Frequency(×100Hz)
1	17, 19, 21, 23, 25	6
2	21	2, 4, 6, 8, 10, 20

Table 3. The machining parameters used in the machining microgroove experiment.

Group	Voltage(V)	Frequency(×100Hz)	Feed speed(μm/s)	Rotation speed(×100rpm)
1	17, 19, 21, 23, 25	6	7	6

2	21	1, 2, 4, 6, 8, 10	7	6
3	21	6	3, 5, 7, 9, 11, 13	6
4	21	6	7	1, 2, 4, 6, 8, 10

When processing microgrooves and 3D microstructures, it is not suitable for the processing method of gravity feed, so we used uniform feed. When the microgrooves became deeper, it is difficult for the electrolyte to enter the bottom of the processing area, making processing difficult to continue. Cutting from the side of the workpiece can effectively avoid this situation. This method can make the electrolyte easily enter the processing area and ensure continuous spark discharge. And this method is more conducive to the discharge of machining chips, thereby improving machining accuracy [31]. The machining parameters used in the machining microgroove experiment are shown in Table 3.

Before each experiment, preload the power supply for 2 minutes ECDM to raise the temperature of the electrolyte, so the following experiment can reach a stable and balanced state [32]. Use the current probe to collect the current signal, and display the waveform of the collected signal through the oscilloscope. Besides, every experiment repeated 5 times under the same parameter conditions to reduce the experiment error. Then average the experiment results.

After the processing completed, the surface morphology of the micro-holes, the surface morphology of the microgrooves and the 3D morphology of the processed workpiece observed and photographed by a scanning electron microscope (SEM). Glass does not conduct electricity, it cannot observe directly through an SEM, so a layer of gold or carbon film must spray on the workpiece, so the workpiece material can observe under the SEM. The contour of the bottom surface of microgrooves measured and calculated using a SURFCOM130A roughness meter.

3. Results and discussion

3.1The influence of different experimental parameters on micro-holes processing

In the Group 1 micro-hole experiment, fix the power frequency at 600Hz and the set the voltage at 17V, 19V, 21V, 23V and 25V respectively. Record the processing depth every 10 seconds (S) during the processing, and set the total processing time to 60 S. Figure 3 shows the relationship between micro-holes MRR and power supply voltage. The MRR is the difference of the processing depth recorded in two adjacent times divided by the time period (10 seconds). That is, the slope *k* in Fig.3.

The results show the MRR increased as the voltage increased. Increase in applied voltage increases the MRR due to generation of more hydrogen gas bubbles resulting in greater amount of discharge energy at the sparking zone. When the voltage increased, the gas layer formation time significantly shortened with the increase in the applied voltage. As the voltage increased, the number and speed of bubble generation increased, so the gas layer formation time significantly shortened, the power of spark discharge increased, and the MRR increased. Besides, the bubbles produced by the electrolysis reaction increased, the gas layer formed faster and more stable, the frequency of discharge increased, and the MRR also improved.

The results also show that the changing trends of MRR under different voltages were similar: they were all the largest in the initial time, and then the MRR remained basically unchanged after reducing to a certain value. (That is, the slope *k* of the line in Figure 3 was basically unchanged after 10 seconds). As the depth of the micro-hole increased, electrolyte became more difficult to circulate in the hole, which reduced the frequency of discharge at the electrode tip. So, the difference between different MRR under various voltage conditions decreased.

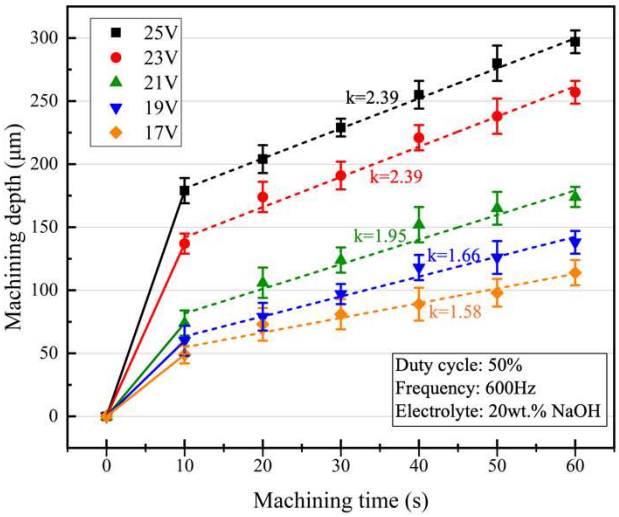

Figure 3. Effect of power voltage on micro-hole MRR.

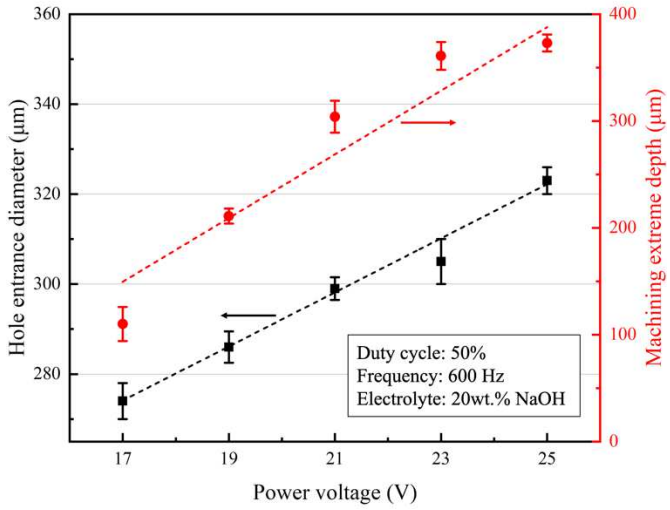

Figure 4. The effect of power voltage on hole entrance diameter and limiting depth.

Figure 4 shows the relationship between the hole entrance diameter and the hole limiting depth with the power supply voltage. In ECDM, the specified work material can be machined only up to a certain depth known as the limiting depth for a particular combination. The potential difference between the tool-electrode and the electrolyte decreases during the process as the tool keeps penetrating inside the work. This potential loss is mainly due to accumulation of gas bubbles on the tool-electrode that restricts the electrolyte flow to the tip of the tool-electrode, which results in reduction of discharge activity and lowering chemical etching. The results show that as the voltage increased, the hole entrance diameter had a significant increase. On the one hand, during the ECDM, discharge also occurred on the side of the electrode, which could increase the diameter of micro-holes. And we noted plenty number of bubbles at holes entrance, which also caused the discharge in this area denser, and made the diameter of the entrance increase. On the other hand, during the machining process, as the power supply voltage increased, the power of the discharge increased, which increased the heat removal of the material. During processing, discharge occurred at holes' entrance. The higher the voltage, the longer the duration of discharge machining in a single pulse period, so the more material removed at holes' entrance. The increase in the diameter of holes facilitates to circulate the electrolyte in holes, thereby promoting the increase in the limit depth of the processed holes, as shown in Figure 4.

Figure 5 shows the micro-holes entrance morphology when the power supply voltage was 21V, 23V and 25V respectively. When the voltage is 21V, the morphology and roundness of the hole are better. The higher the voltage, the more obvious defects such as micro-cracks and pits at holes entrance. Because spark discharge produced in the form of pulse. During discharge, the material near the spark heated and expanded. When the pulse finished, this part of the material contacted the lower temperature electrolyte and cooled and shrank. At holes entrance, the electrolyte is enough and the frequency of spark discharge is high, so that the material at holes entrance continuously expands and shrinks. Under the effect of continuous thermal expansion and contraction, winkle-like defects would occur on the processed surface. When the voltage become higher, not only the energy produced by the spark discharge will increase, but the frequency of discharge also increased. Further, this intensifies the frequency of thermal expansion and contraction of the material, causing cracks and pits. At the same time for high voltage, some cracks will be produced in the machining zone due to excessive heat generation. With further increase in applied voltage, these cracks may propagate and lead to the total rapture of the workpiece. Eventually, the entire piece of material will fall off, forming pits and other defects.

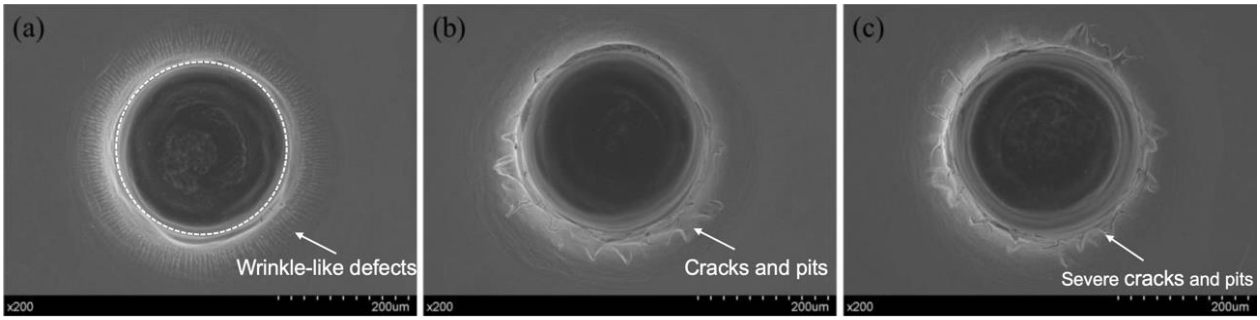

Figure 5. Micro-hole entrance morphology processed at the power voltage of (a) 21V, (b) 23V and (c) 25V.

In the Group 2 micro-hole experiment, fix the power voltage at 21V and the set the frequency at 200Hz, 400Hz, 600Hz, 800Hz, 1000Hz and 2000Hz respectively. Record the processing depth every 10 S during the processing, and set the total processing time to 60 S. Figure 6 shows the relationship between micro-holes MRR and power frequency. Figure 6 shows similar features to Figure 3. In the early stage of processing, the change of power frequency had a greater impact on MRR, and low-frequency processing had higher MRR. When the power frequency reduced, the total time of gas layer formation becomes shorter and the stable spark discharge time is longer. Therefore, the MRR was higher. As

the processing time increased, the MRR at different frequency was similar. The initial MRR was higher, and the machining depth was deeper in a short time. However, as the depth increases, circulating the electrolyte in the hole becomes difficult, which increases the difficulty of spark discharge at the electrode end, so the MRR also decreased.

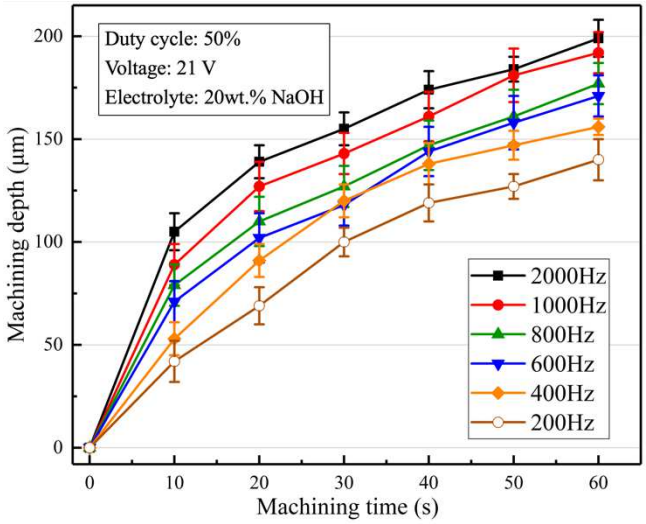

Figure 6. Effect of power frequency on micro-hole machining efficiency.

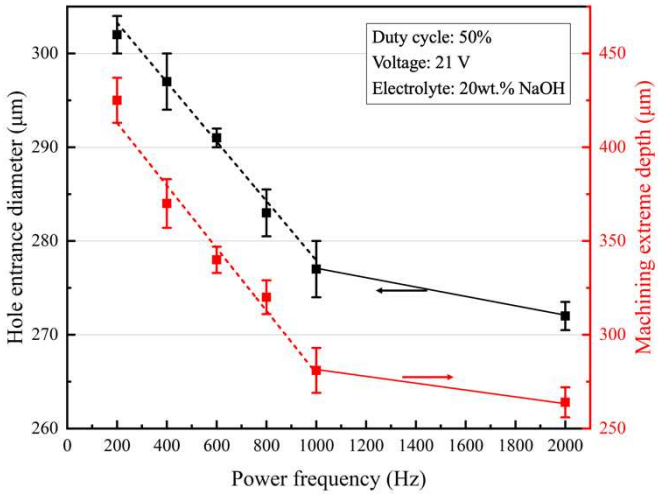

Figure 7. The effect of power frequency on hole entrance diameter and machining extreme depth.

Figure 7 shows the relationship between hole entrance diameter and hole limiting depth with power frequency. The results show that the higher the power frequency, the smaller the entrance diameter. When the power frequency is high, the spark discharge position will be smaller. A single pulse period includes gas film formation time and discharge time. As the frequency of the power supply increases, the number of pulses per unit time increases, that is, the number of discharges increases, and the more gas film formation time is required. Therefore, the smaller the proportion of the system for spark discharge in the same time. Therefore, the less material removed by heating, the smaller the hole size. The results also show that the limiting depth decreased with the increase of frequency. With the increase of power frequency, the diameter of micro-holes decreased. The smaller the diameter, the more unfavorable the electrolyte circulation in the hole, thus limiting the increase of the limiting depth of the hole.

The change of the power frequency also has a great influence on the morphology of micro-holes entrance. Figure 8 shows the micro-hole entrance morphology machined using 200Hz, 400Hz, 600Hz and 800Hz power frequency. The figure shows that when the frequency is 600 Hz, the morphology and roundness of the hole are better. When the frequency is lower than 600 Hz, the action time of every single spark is longer. So, the heat accumulation effect is obvious, which could cause the material around the hole to melt and remove in lumps, as shown in Figure 8a-b. When the frequency is greater than 600 Hz, the rapid thermal expansion and contraction result in a dense line (wrinkle-liked defects) around the hole entrance, as shown in Figure 8d.

According to the micro-hole experiment, the parameters selected as the power supply voltage 21V and the frequency 600Hz for processing. Figure 9 shows the micro-holes processed in this parameter optimization. The figure shows that no obvious defects such as cracks at the entrance, the processing repeatability is good, and holes have good roundness, so the selected parameters are reasonable.

This section carried out the experiment of electrochemical discharge micro-hole processing. This study analyzed the influence of voltage and frequency on micro-hole machining. Through experimental comparison, we selected reasonable processing power parameters (voltage 21V, frequency 600Hz), which can achieve higher MRR and deeper holes. This experiment got smaller holes entrance diameter and better surface quality.

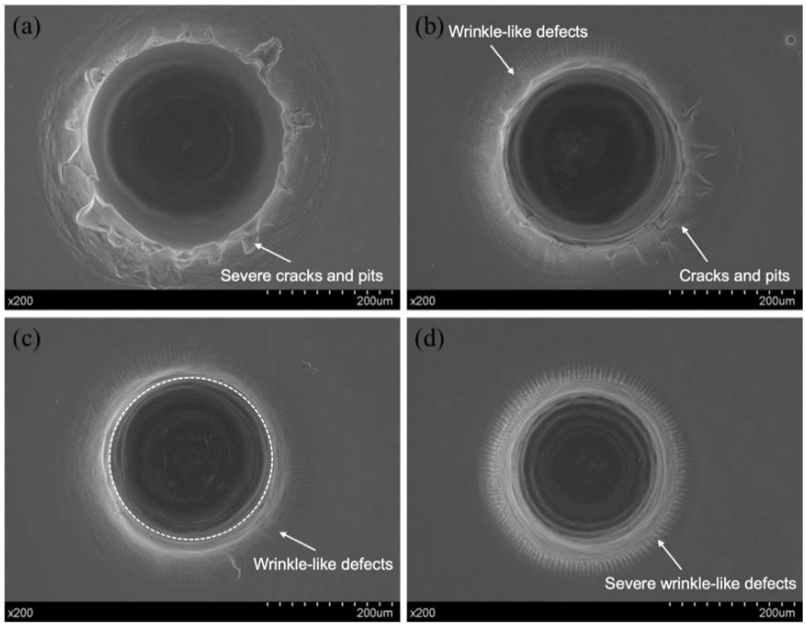

Figure 8. Micro-hole entrance morphology processed at the power frequency of (a) 200Hz, (b) 400Hz, (c) 600Hz and (d) 800Hz.

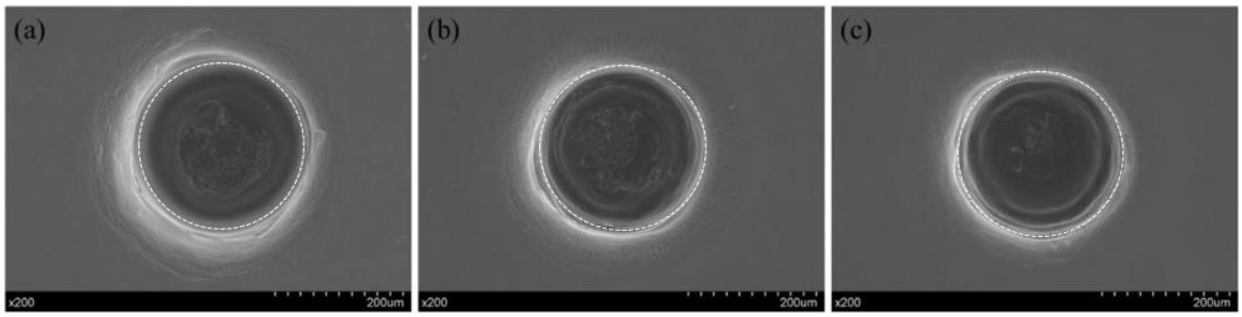

Figure 9. Micro-holes with good roundness, good surrounding quality and high repeatability-processed with optimized parameters.

3.2 The influence of different experimental parameters on the roughness of microgrooves

This section mainly discussed the influence of four factors of power supply voltage, power supply frequency, tool electrode feed rate and tool electrode rotation speed on the surface roughness of microgrooves by ECDM. Figure 10 shows the SEM images of microgrooves processed with different parameters. Below the microgrooves is the bottom surface roughness. The sampling length in the test is 500 μm, The sampling location for roughness measurement is the bottom of the microgroove, and the sampling length is 500 μm. The surface roughness values in the figure were 0.742 μm and 0.409 μm, respectively.

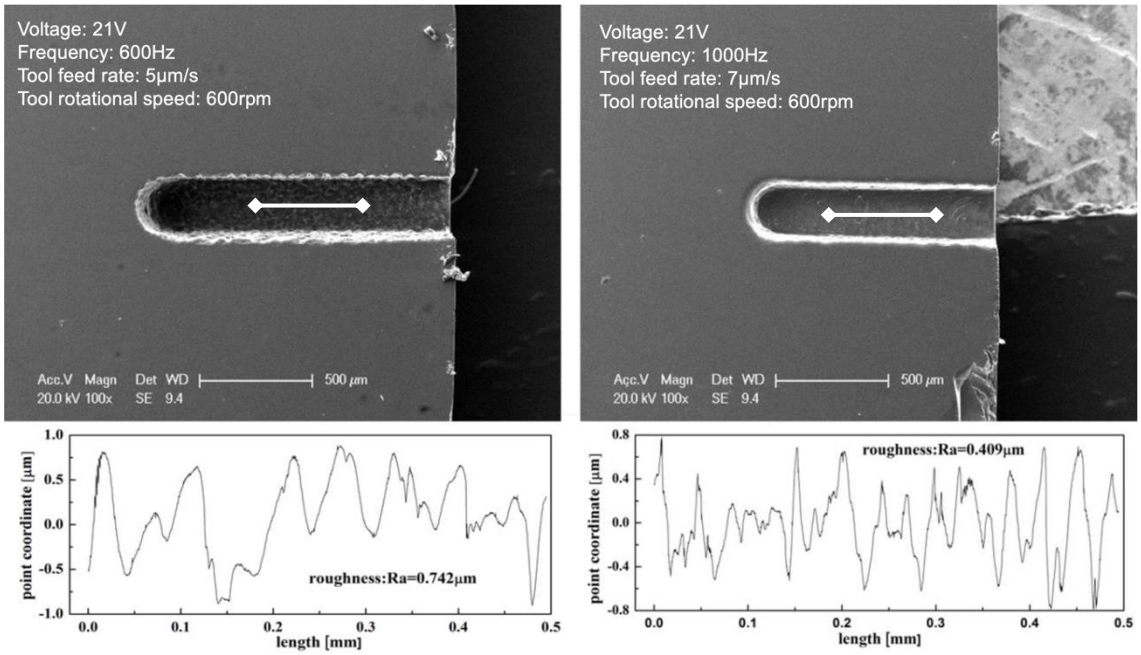

Figure 10. SEM images and roughness measurement of microgrooves.

Figure 11 shows the relationship of microgroove roughness with power supply voltage, power supply frequency, electrode feed speed and electrode rotation speed. The roughness value of the microgrooves had an obvious linear with the power supply voltage, power supply frequency and electrode feed rate, but had no clear linear relationship with the electrode rotation speed. The roughness value of the microgrooves increased with the increase of the voltage. When the power supply voltage increases, the average spark discharge current increased, so the energy of the spark discharge pulse also increased; and the increase of the voltage will also increase the frequency of the spark discharge, so the total heat produced became larger. The thermal influence of the machined surface was also greater, causing the surface quality to decrease and the roughness value to increase.

The roughness value decreased as the electrode feed rate increases. Very low feed rates will increase machining time and tend to increase the HAZ around the machined area. As the feed rate increases, the time required for the electrode to pass through the same point on the surface of the workpiece decreases, so the thermal effect of spark discharge at this point also reduced, and the roughness correspondingly reduced. However, too high a feed rate will also cause mechanical contact between the electrode and the workpiece surface. The feed rates faster than the mean material removal rate of the process may lead to failure of either the workpiece or the tool electrode. Therefore, the feed rate should not be too large during processing.

Figure 11 (d) shows that the roughness value varied from 0.605μm to 0.719μm, but it did not change regularly with the electrode speed. Before the rotation speed reached 600 rpm, the rotation speed of the electrode surface of the threaded tool was too low to provide the centripetal force to form a dense air film, so the roughness is not significantly improved. After 600 rpm, the roughness tended to improve as the rotation speed increases. After the speed reached a certain value, sufficient centripetal force was provided, and the air film was relatively stable.

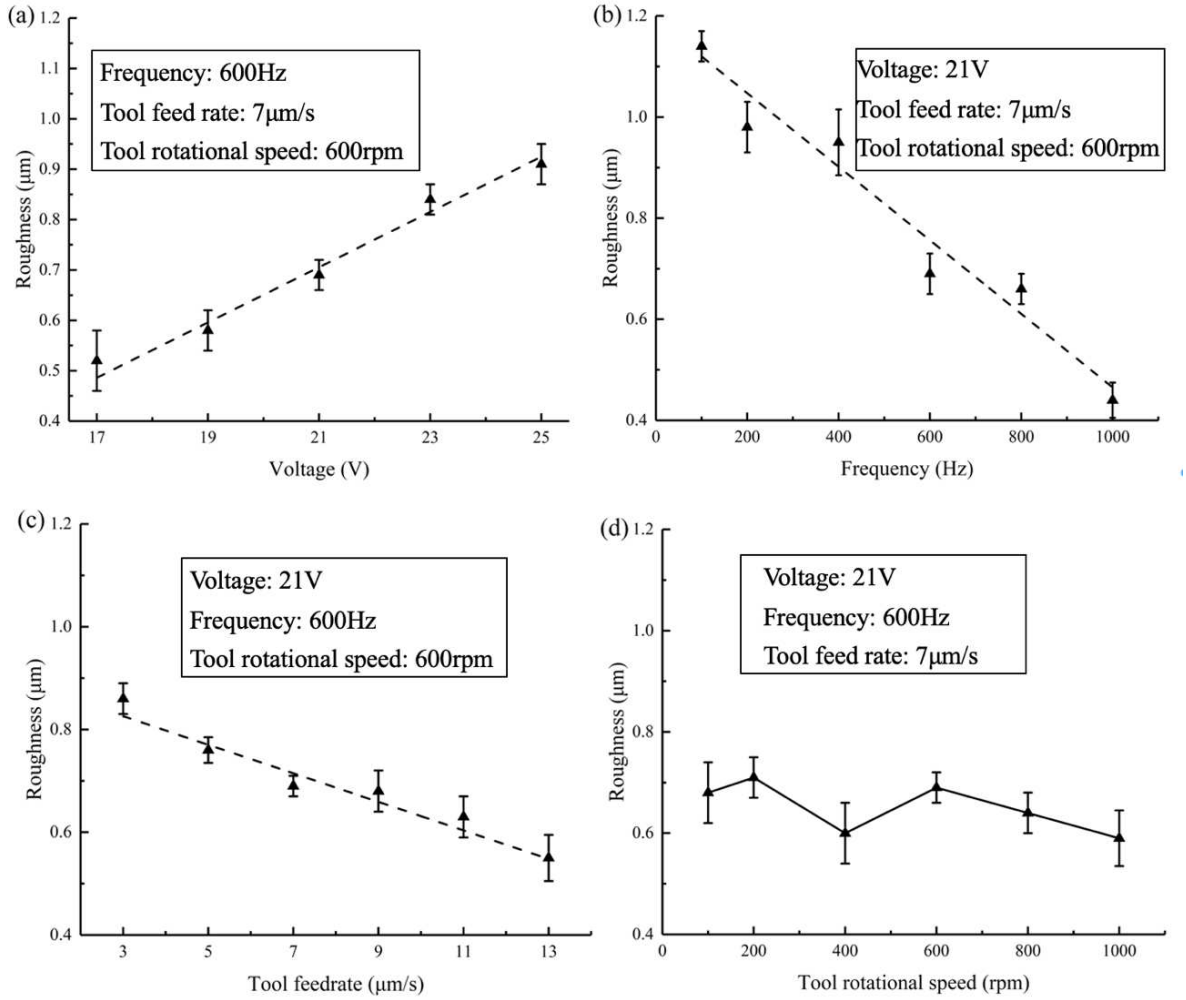

Figure 11. Effect of (a)voltage (b)frequency (c)tool feed rate (d)tool rotational speed on roughness.

3.3 Machining 3D microstructure

For microgrooves with high aspect ratios, scholars usually adopt a layer-by-layer processing method [31]. Because when the depth of the microgrooves processed in a single time is deep, it is easy to cause mechanical contact between the tool electrode and the workpiece, which causes obvious defects such as cracks on the processed surface of the workpiece. More serious will cause the tool electrode to break due to excessive contact force. In this experiment, considering the results of micro-hole machining and microgroove machining, considering the machining quality and machining efficiency, we selected the machining parameters as power supply voltage 21V, pulse frequency 600Hz, electrode rotation speed 1000rpm and electrode feed rate of 7μm/s. And the 3D microstructure on the glass was processed by layer, with each layer feeding 100 μm. Figure 12 shows the 3D microstructures machined with the optimum parameters an 3D image of one of them. The results show that the 3D microstructures processed by the optimized parameters were smooth without cracks and wrinkle-liked defects.

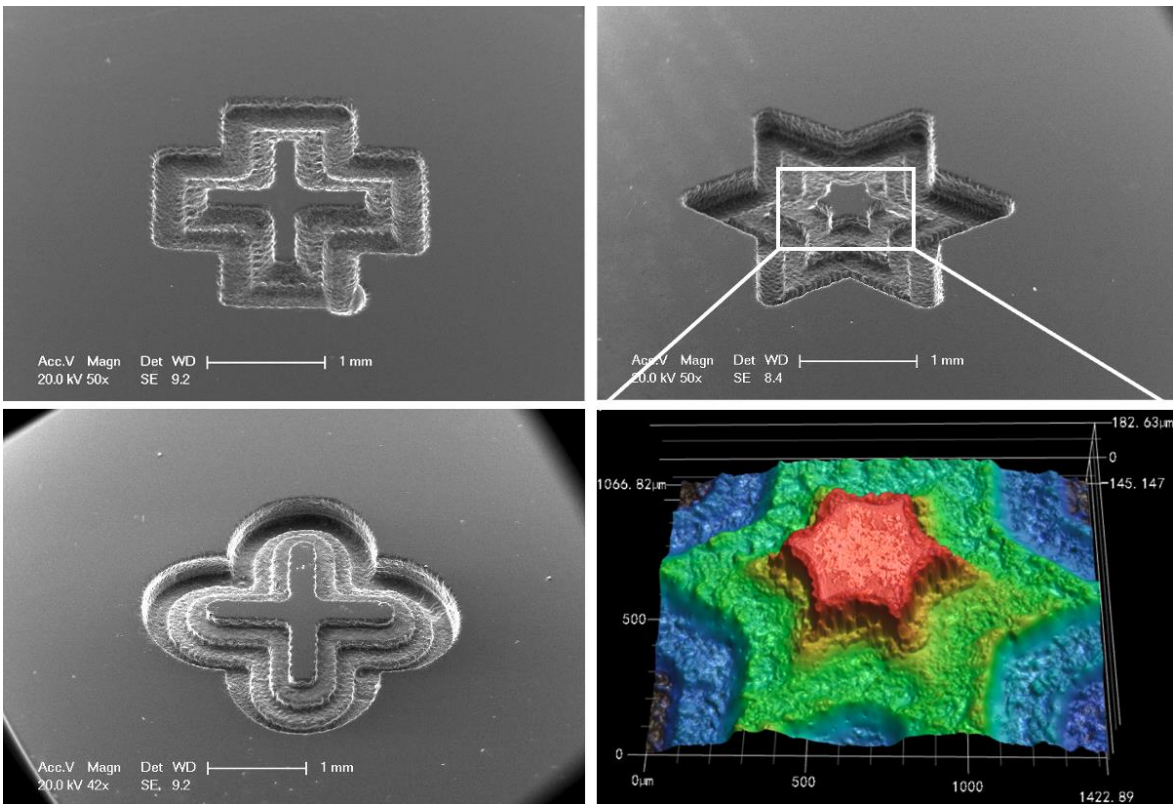

Figure 12. 3D microstructures machined by optimized parameters (power supply voltage 21V, pulse frequency 600Hz, electrode rotation speed 1000rpm and electrode feed rate of 7μm/s).

4. Conclusions

This paper carried out ECDM experiments of micro-holes, microgrooves and 3D microstructures on glass. Appropriate machining methods selected to discuss the variation of machining efficiency and machining quality with different machining parameters. Compared with the existing research, this paper systematically studies the power supply voltage, frequency, electrode rotation speed and electrode feed rate. The experiments of micro-hole (one-dimensional), micro-groove (two-dimensional) and three-dimensional machining were gradually carried out. The experimental results of micro-holes and micro-grooves are emphatically evaluated, focusing on the processing efficiency of micro-holes and the degree of over-cutting, and the roughness of micro-grooves is used as a measurement standard, and the optimal parameters are selected for the final three-dimensional processing. The conclusion is as follows:

1. In micro-hole machining, increasing the power supply voltage can increase the energy of spark discharge, thereby improving machining efficiency and increasing the limit depth of micro-holes. But it will bring the increase of the entrance diameter and the deterioration of the entrance morphology. Choosing a lower power frequency will correspondingly shorten the time required for gas layer formation and prolong the duration of spark discharge, thereby improving processing efficiency and increasing the limit processing depth of micro-holes. However, the lower frequency also increased the entrance diameter and the entrance morphology was worse. A power supply voltage of 21V and a power supply frequency of 600Hz comprehensively selected as processing parameters.
2. In microgroove machining, the roughness of the microgrooves was directly proportional to the power supply voltage, inversely proportional to the power supply frequency and the feed speed of the tool electrode, but had no obvious relationship with the electrode speed. Comprehensive comparison found that the selected voltage and frequency parameters are reasonable, and the electrode rotation speed of 1000 rpm and the electrode feed speed of 7 μm/s selected as the processing parameters.
3. Selecting reasonable processing parameters and adopting a layer-by-layer processing method can consider processing quality and processing efficiency to obtain complex 3D microstructures.

Acknowledgements

This work was supported by National Natural Science Foundation of China, grant number 52075227, 51905226; China Postdoctoral Science Foundation 2018M640461, 2019T120392; Natural Science Foundation of Jiangsu Province, grant number BK20180873, BK20180875; Postgraduate Research & Practice Innovation Program of Jiangsu Province 5561110037.

References

[1] Wang ZK, Zheng HY, Seow WL, Wang XC. Investigation on material removal efficiency in debris-free laser ablation of brittle substrates. J Mater Process Technol 2015;219:133–42. https://doi.org/https://doi.org/10.1016/j.jmatprotec.2014.12.013.

[2] Huang Y-X, Lu J-Y, Huang J-X. KrF excimer laser precision machining of hard and brittle ceramic biomaterials. Biomed Mater 2014;9:35009. https://doi.org/10.1088/1748-6041/9/3/035009.

[3] Zhu H, Zhang Z, Zhou J, Xu K, Zhao D, Tangwarodomnukun V. A computational study of heat transfer and material removal in picosecond laser micro-grooving of copper. Opt Laser Technol 2021;137. https://doi.org/10.1016/j.optlastec.2020.106792.

[4] Kim HJ, Lee SH, Lee J, Lee ES, Choi JH, Jung JY, et al. Controlled patterning of vertical silicon structures using polymer lithography and wet chemical etching. J Nanosci Nanotechnol 2015;15:4522–9. https://doi.org/10.1166/jnn.2015.9780.

[5] Nath C, Lim GC, Zheng HY. Influence of the material removal mechanisms on hole integrity in ultrasonic machining of structural ceramics. Ultrasonics 2012;52:605–13. https://doi.org/10.1016/j.ultras.2011.12.007.

[6] Bhattacharyya B, Doloi BN, Sorkhel SK. Experimental investigations into electrochemical discharge machining (ECDM) of non-conductive ceramic materials. J Mater Process Technol 1999;95:145–54.

[7] Goud M, Sharma AK, Jawalkar C. A review on material removal mechanism in electrochemical discharge machining (ECDM) and possibilities to enhance the material removal rate. Precis Eng 2016;45:1–17. https://doi.org/10.1016/j.precisioneng.2016.01.007.

[8] Zhang Z, Huang L, Jiang Y, Liu G, Nie X, Lu H, et al. A study to explore the properties of electrochemical discharge effect based on pulse power supply. Int J Adv Manuf Technol 2016;85:2107–14. https://doi.org/10.1007/s00170-015-8302-9.

[9] Zhao D, Zhang Z, Zhu H, Cao Z, Xu K. An investigation into laser-assisted electrochemical discharge machining of transparent insulating hard-brittle material. Micromachines 2021;12:1–12. https://doi.org/10.3390/mi12010022.

[10] Arab J, Dixit P. Influence of tool electrode feed rate in the electrochemical discharge drilling of a glass substrate. Mater Manuf Process 2020;00:1–12. https://doi.org/10.1080/10426914.2020.1784936.

[11] Kurafugi H, Suda H. Electrical discharge drilling of glass. CIRP Ann - Manuf Technol 1968;16.

[12] Tokura H, Kondoh I, Yoshikswa M. Ceramic material processing by electrical discharge in electrolyte. J Mater Sci 1989;24:991–8.

[13] Vogt H. Contribution to the interpretation of the anode effect. Electrochim Acta 1997;42:2695–705.

[14] Hajian M, Razfar MR, Movahed S. An experimental study on the effect of magnetic field orientations and electrolyte concentrations on ECDM milling performance of glass. Precis Eng 2016;45:322–31. https://doi.org/10.1016/j.precisioneng.2016.03.009.

[15] Elhami S, Razfar MR. Analytical and experimental study on the integration of ultrasonically vibrated tool into the micro electro-chemical discharge drilling. Precis Eng 2017;47:424–33. https://doi.org/10.1016/j.precisioneng.2016.09.015.

[16] Wüthrich R, Spaelter U, Bleuler H. The current signal in Spark Assisted Chemical Engraving (SACE), what does it tell us ? J Micromechanics Microengineering 2006;16:779.

[17] Wüthrich R, Fascio V. Machining of non-conducting materials using electrochemical discharge phenomenon - An overview. Int J Mach Tools Manuf 2005;45:1095–108. https://doi.org/10.1016/j.ijmachtools.2004.11.011.

[18] Cheng CP, Wu KL, Mai CC, Yang CK, Hsu YS, Yan BH. Study of gas film quality in electrochemical discharge machining. Int J Mach Tools Manuf 2010;50:689–97. https://doi.org/10.1016/j.ijmachtools.2010.04.012.

[19] Jawalkar CS, Sharma AK, Kumar P. Investigations on performance of ECDM process using NaOH and NaNO 3 electrolytes while micro machining soda lime glass. Int J Manuf Technol Manag 2014;28:80–93.

[20] Zheng ZP, Cheng WH, Huang FY, Yan BH. 3D microstructuring of Pyrex glass using the electrochemical discharge machining process. J Micromechanics Microengineering 2007;17:960–6. https://doi.org/10.1088/0960-1317/17/5/016.

[21] Paul L, Korah L V. Effect of Power Source in ECDM Process with FEM Modeling. Procedia Technol 2016;25:1175–81. https://doi.org/10.1016/j.protcy.2016.08.236.

[22] Jui SK, Kamaraj AB, Sundaram MM. High aspect ratio micromachining of glass by electrochemical discharge machining (ECDM). J Manuf Process 2013;15:460–6. https://doi.org/10.1016/j.jmapro.2013.05.006.

[23] Abou Ziki JD, Fatanat Didar T, Wüthrich R. Micro-texturing channel surfaces on glass with spark assisted chemical engraving. Int J Mach Tools Manuf 2012;57:66–72. https://doi.org/10.1016/j.ijmachtools.2012.01.012.

[24] Singh T, Dvivedi A. On performance evaluation of textured tools during micro-channeling with ECDM. J Manuf Process 2018;32:699–713. https://doi.org/10.1016/j.jmapro.2018.03.033.

[25] Singh T, Dvivedi A. On pressurized feeding approach for effective control on working gap in ECDM. Mater Manuf Process 2018;33:462–73. https://doi.org/10.1080/10426914.2017.1339319.

[26] Fascio V, Wüthrich R, Bleuler H. Spark assisted chemical engraving in the light of electrochemistry. Electrochim Acta 2004;49:3997–4003.

[27] Jalali M, Maillard P, Wüthrich R. Toward a better understanding of glass gravity-feed micro-hole drilling with electrochemical discharges. J Micromechanics Microengineering 2009;19. https://doi.org/10.1088/0960-1317/19/4/045001.

[28] Salonitis K, Stournaras A, Stavropoulos P, Chryssolouris G. Thermal modeling of the material removal rate and surface roughness for die-sinking EDM. Int J Adv Manuf

Technol 2009;40:316–23.
[29] Razfar MR, Behroozfar A, Ni J. Study of the effects of tool longitudinal oscillation on the machining speed of electrochemical discharge drilling of glass. Precis Eng 2014;38:885–92. https://doi.org/10.1016/j.precisioneng.2014.05.004.
[30] Cao XD, Kim BH, Chu CN. Hybrid micromachining of glass using ECDM and micro grinding. Int J Precis Eng Manuf 2013;14:5–10. https://doi.org/10.1007/s12541-013-0001-6.
[31] Kolhekar KR, Sundaram M. Study of Gas Film Characterization and its effect in Electrochemical Discharge Machining. Precis Eng 2018:S0141635917307614.
[32] Paul L, Kurian G. Effects of Preheating Electrolyte in Micro ECDM Process. vol. 5. 2018.